

Mediator-free microfluidics biosensor based on titania-zirconia nanocomposite for urea detection

Cite this: *RSC Advances*, 2013, 3, 228

Saurabh Srivastava,^{ab} Md. Azahar Ali,^a Pratima R. Solanki,^a Pandurang M. Chavhan,^a Manoj K. Pandey,^a Ashok Mulchandani,^c Anchal Srivastava^b and Bansi D. Malhotra^{*d}

Urease (Urs) and glutamate dehydrogenase (GLDH) co-immobilized onto titania-zirconia (TiO₂-ZrO₂) nanocomposite and integrated with microfluidics mediator-free sensor have been utilized for urea detection. The PDMS microchannels have been sealed with a glass substrate comprising of reference (Ag/AgCl), counter (ITO) and working (Urs-GLDH/TiO₂-ZrO₂/ITO) electrodes. This mediator-free microfluidics urea sensor shows linearity as 5–100 mg/dL with improved sensitivity as 2.74 μA [Log mM]⁻¹ cm⁻² and detection limit of 0.07 mg/dl (0.44 mM) using 3σ_b/m criteria. The Reynolds number has been found to be as 0.166, indicating that fluid flow is completely laminar, controllable and the pressure drop across the microchannels is found to be as 3.5 × 10³ Pa.

Received 16th July 2012,
Accepted 24th October 2012

DOI: 10.1039/c2ra21461j

www.rsc.org/advances

Introduction

Recent years have seen increased interest towards the development of miniaturized microfluidics biosensing devices. In a microfluidics system, the integration of microchannels provides novel functions because of smart geometries and controllable dimensions that offer complete functional devices such as lab-on-a-chip¹ for enzymatic analysis,² immunoassays³ and capillary electrophoresis⁴ *etc.*

The potential applications of microfluidics devices have led to increased demand due to low consumption of reagents, short reaction time and design flexibility. Polydimethylsiloxane (PDMS) is known to be an interesting polymer for microfluidics device fabrication due to remarkable elasticity, optical transparency, simple and low cost.⁵ The electrochemical techniques are currently one of the most commonly used detection methods because of the high sensitivity and fast response time for desired microfluidics module.⁶

There is increased interest towards the fabrication of nanostructured metal oxides (NMOs) including titanium dioxide (TiO₂) and zirconium dioxide (ZrO₂) for clinical diagnostics^{7–9} due to higher surface-to-volume ratio, high

isoelectric point, non-toxicity, chemical stability, biocompatibility and high electron transfer ability.^{10–12}

The estimation of urea is important for clinical analysis, since increased urea level in blood and urine causes various kidney diseases.^{13–15} We report results of the studies relating to development of mediator-less microfluidics device based on TiO₂-ZrO₂ nanocomposite for urea detection. It is found that presence of this binary oxide facilitates direct electron transfer between active sites of the enzymes to the electrode. It has been reported that addition of ZrO₂ to TiO₂ can prevent phase transformation from anatase to rutile, lead to enhanced catalytic, photocatalytic and electrochemical properties due to modification in electronic band structure and interfacial state.^{16–18} To the best of our knowledge, we are reporting for the first time a TiO₂-ZrO₂ nanocomposite incorporated mediator-free microfluidics sensor for urea detection.

Experimental section

2.1 Chemicals

All chemicals have been procured from Sigma Aldrich. Sylgard 184 is procured from Dow Corning (Midland, MI, USA). SU-8-100 negative photoresist and SU-8 developer have been acquired from Microchem (Newton, MA, USA).

2.2 Synthesis of TiO₂-ZrO₂ nanocomposite

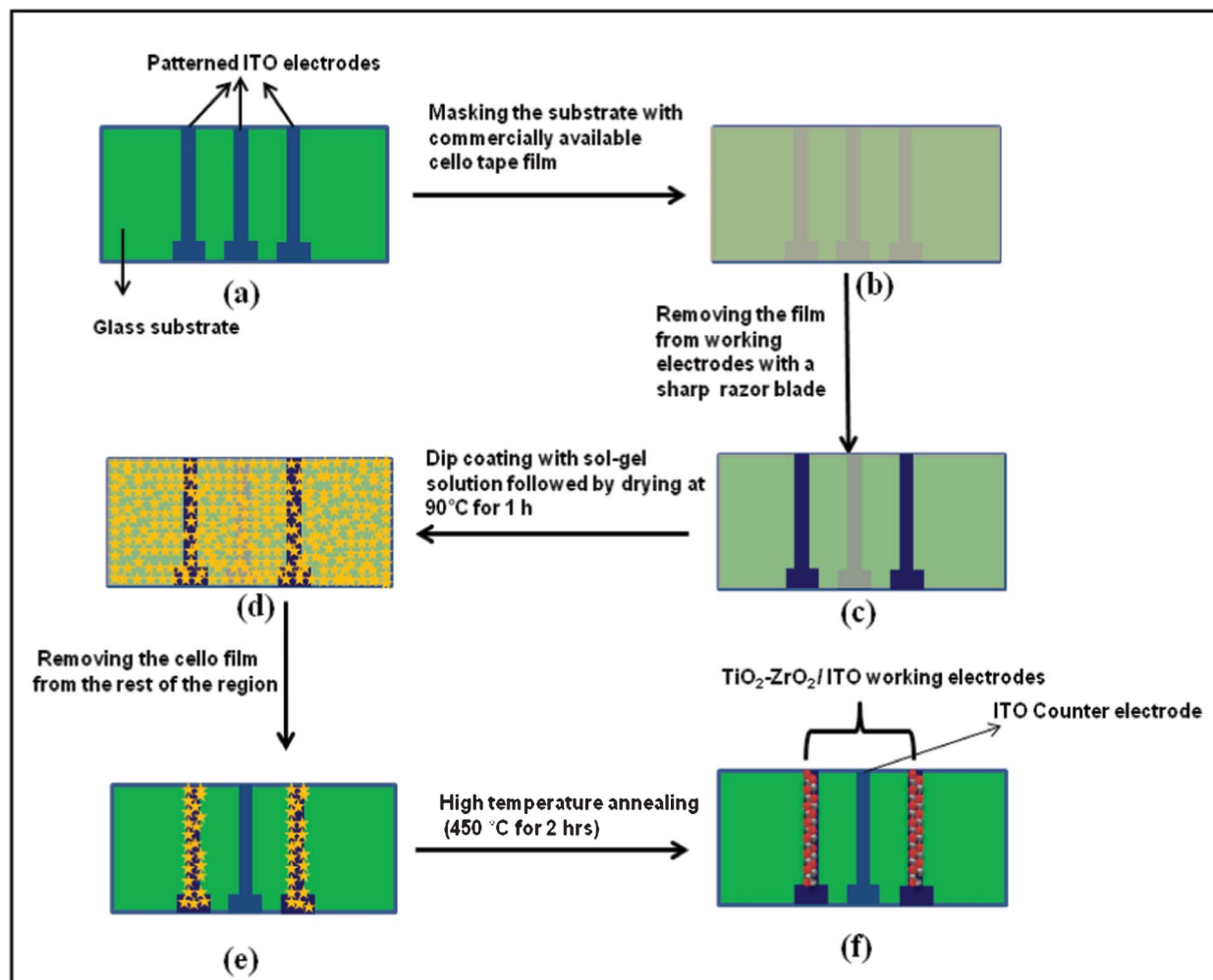
Zirconium (IV) n-propoxide and titanium(IV) butoxide (1 : 1 molar ratio) are dissolved in 2-methoxy ethanol to prepare 5(wt%) precursor sol solution and hydrolyzed by drop wise addition of 500 μl of H₂O and nitric acid (25 μl of 70%) under

^aDepartment of Science and Technology Centre on Biomolecular Electronics, Biomedical Instrumentation Section, National Physical Laboratory, New Delhi, 110012, India

^bDepartment of Physics, Banaras Hindu University, Varanasi, 221005, UP, India

^cDepartment of Chemical and Environmental Engineering, University of California, Riverside, CA, 92521, USA

^dDepartment of Biotechnology, Delhi Technological University, Main Bawana Road, Delhi, 110042, India. E-mail: bansi.malhotra@gmail.com; Tel: 91-11-27871043 (Ext-1609)



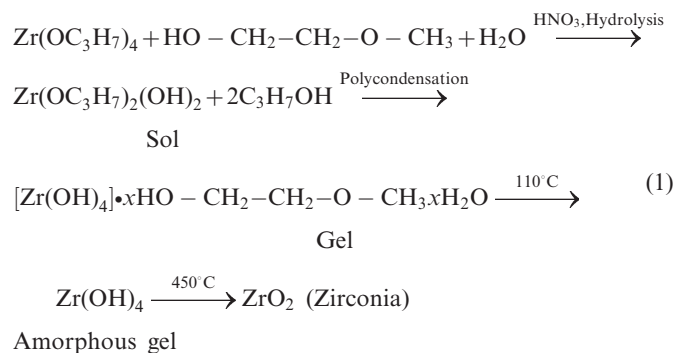
Scheme 1 The process of modifying only the working ITO electrode (WE1 and WE 2) with $\text{TiO}_2\text{-ZrO}_2$ nanocomposite using the dip coating method is shown.

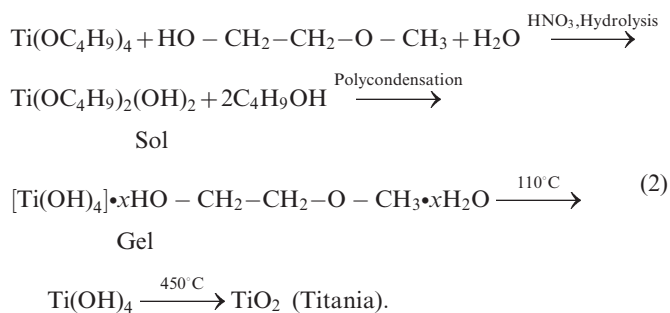
continuous stirring followed by keeping for about 2 h at 25 °C for ageing.

2.3 Fabrication of microfluidics electrodes and microchannels

Two patterned microelectrodes comprising of dimensions ($0.2 \times 2.5 \text{ cm}^2$) are fabricated onto indium tin oxide (ITO) coated glass slide ($2.5 \times 3.5 \text{ cm}^2$) by wet chemical etching process. The working electrodes (WE 1 and WE 2) are used to deposit $\text{TiO}_2\text{-ZrO}_2$ nanocomposite film by dip coating method (Scheme 1). For this process, first we take the glass substrate containing three patterned ITO electrodes (step a, Scheme 1) that is masked with commercially available cello tape film (step b). We then remove the cello tape from the two patterned ITO electrodes using a sharp razor blade (step c), leaving central ITO microelectrode and the substrate remains covered. This substrate is dip coated with transparent sol-gel solution followed by drying at 90 °C for 1 h (step d). The remaining cello tape film is then removed from the rest of the substrate. The dried sol-gel film onto patterned ITO electrodes is finally annealed at 450 °C for 2 h to obtain $\text{TiO}_2\text{-ZrO}_2$

nanocomposite (step e). In this process, the central bare patterned ITO electrode remains unmodified with sol-gel coating that is used as the counter electrode. The proposed reactions involved in the synthesis of $\text{TiO}_2\text{-ZrO}_2$ nanocomposite are as follows:





Amorphous gel

2.4 Modification of titanium and zirconium electrode

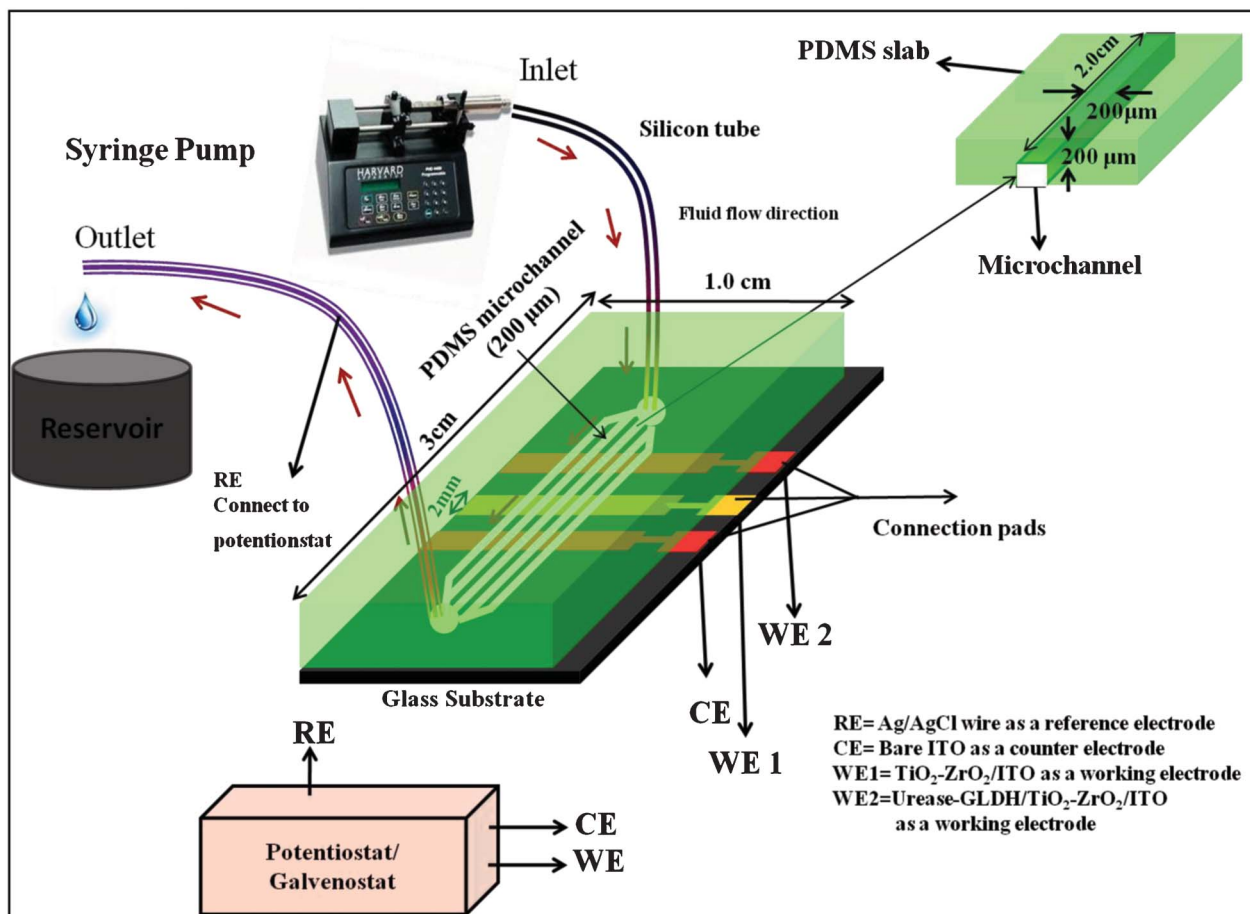
Ten μL of bienzyme [Urease (10 mg mL^{-1}) and GLDH (1 mg mL^{-1})] solutions are spread over $\text{TiO}_2\text{-ZrO}_2/\text{ITO}$ microelectrode by physisorption technique *via* electrostatic interactions and incubated for 3 h at 25°C in humid condition. These bioelectrodes are stored in a refrigerator at 4°C when not in use. The modified $\text{TiO}_2\text{-ZrO}_2/\text{ITO}$ (WE1) and Urs-GLDH/ $\text{TiO}_2\text{-ZrO}_2/\text{ITO}$ (WE2) act as working electrodes whereas a silver wire (0.5 mm dia.) coated with silver chloride (Ag/AgCl) layer is taken as the reference electrode for electrochemical studies.

2.5 Integration of electrode with microfluidics channels

PDMS microchannels have been fabricated using soft lithographic technique and include steps like cleaning of Si wafers, spin coating of photoresist, pre and post exposure heat treatment, UV exposure and development to obtain a positive relief pattern of the photoresist over Si wafers (called Master) of desired dimensions ($2 \text{ cm} \times 200 \mu\text{m} \times 200 \mu\text{m}$).¹⁹ The PDMS oligomer and a cross-linking agent mixed in 10 : 1 are stirred vigorously for about 5 min and are then degassed for about 30 min under vacuum to remove all air bubbles. The clear solution is poured onto the master and heated at 100°C for about 1.5 h. The PDMS layer with pattern of the negative relief is peeled off from the master and cut into suitable size. The reservoirs are fabricated by punching holes at the ends of microchannels. This PDMS chip is tightly clamped with the glass substrate containing ITO microelectrodes, to ensure leakage-free flow operation. The integration of PDMS microchannels and electrodes system for urea detection coupled with electrochemical analyzer is shown in Scheme 2.

2.6 Instrumentation

X-ray diffraction (XRD, Rigaku), atomic force microscopic (AFM, Veeco, Nanoscope) and Fourier transform-infrared (FT-IR, Perkin-Elmer, Model 2000) techniques have been used for



Scheme 2 Schematic representation of microfluidics module for $\text{TiO}_2\text{-ZrO}_2$ nanocomposites based electrochemical urea biosensor.

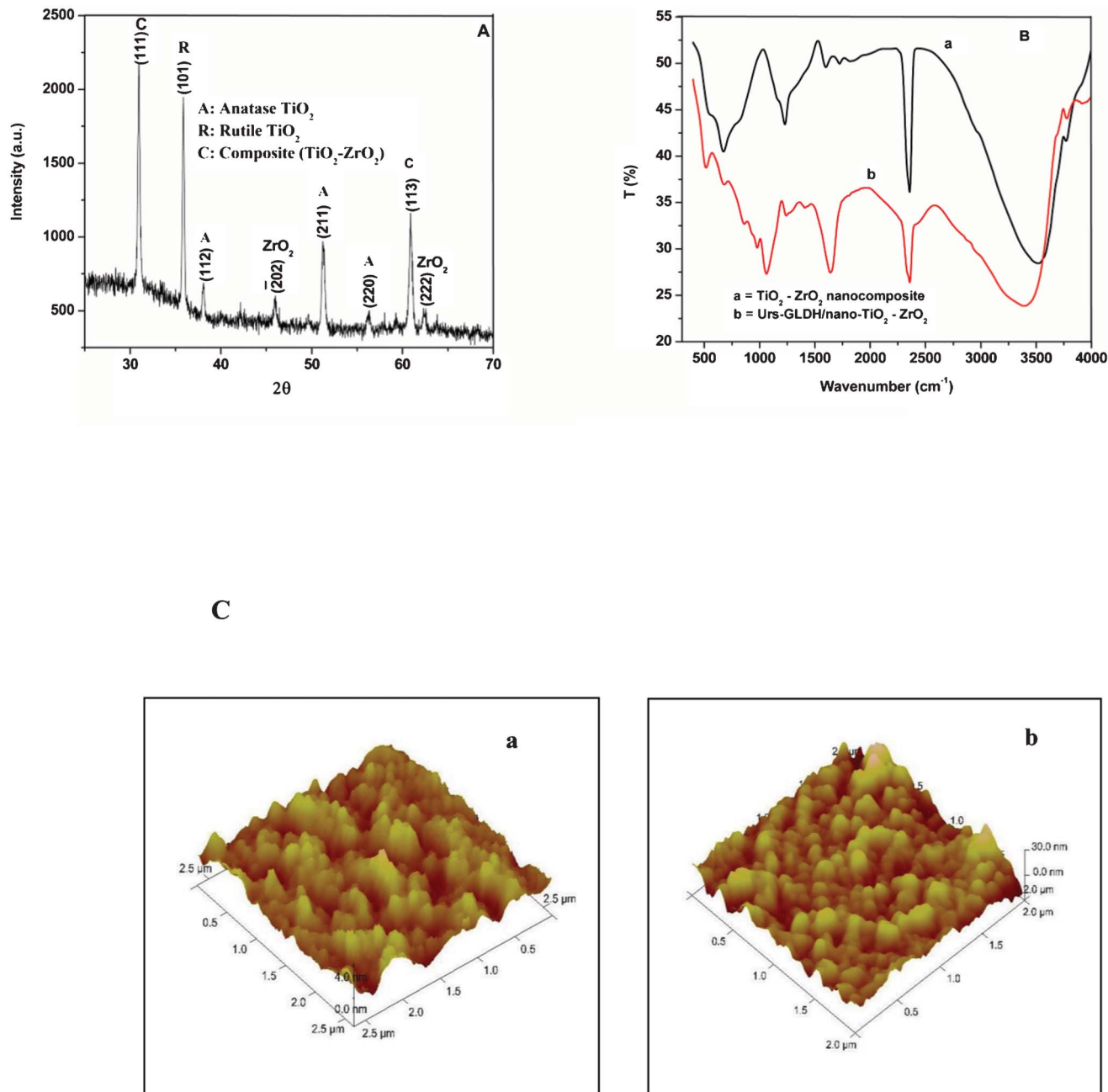


Fig. 1 (A) XRD pattern of TiO₂-ZrO₂ nanocomposite, (B) FTIR spectra of TiO₂-ZrO₂/ITO electrode (a) and Urs-GLDH/TiO₂-ZrO₂/ITO bioelectrode (b), (C) AFM image of TiO₂-ZrO₂/ITO (a) and Urs-GLDH/TiO₂-ZrO₂/ITO (b).

characterization of TiO₂-ZrO₂/ITO electrode and Urs-GLDH/TiO₂-ZrO₂/ITO bioelectrode. Electrochemical studies have been performed in phosphate buffer saline (PBS, pH 7.0 containing 0.9% NaCl) using electrochemical analyzer (Autolab).

Results and discussion

3.1 Structural properties

The XRD pattern of TiO₂-ZrO₂ nanocomposite (Fig. 1A) shows peaks at 2θ: 30.7° and 60.9° corresponding to the diffraction

pattern of (111) and (113) planes indicating the presence of predominant orthorhombic phase of ZrTiO₄ (JCPDS 80-1783). The peak seen at 36° corresponding to (101) plane represents the rutile phase present in TiO₂. The peaks seen at 38°, 51.4° and 56.2° correspond to the diffraction planes (112), (211) and (220) of anatase phase of TiO₂. A small peak found at 62.6° corresponds to (222) plane assigned to cubic crystalline system of ZrO₂ (JCPDS 89-9069). The peak seen at 46° corresponds to (202) reflection plane of ZrO₂ (JCPDS 89-9066). The crystallite size of TiO₂-ZrO₂ nanocomposite calculated using Scherrer formula has been found as 17.8 nm.

3.2 Optical properties

The FT-IR spectra of $\text{TiO}_2\text{-ZrO}_2/\text{ITO}$ nanocomposite [Fig. 1B, (a)] exhibits characteristic peak at 664 cm^{-1} corresponding to vibration bending of Ti-O. A band seen at 740 cm^{-1} is ascribed to ZrTiO_4 species.²⁰ The bands found at 3530 cm^{-1} and 1595 cm^{-1} correspond to the stretching vibration and deformation of the O-H bond due to absorption of the water molecules. The FT-IR spectra of Urs-GLDH immobilized $\text{TiO}_2\text{-ZrO}_2/\text{ITO}$ electrode (b) exhibits band at 1631 cm^{-1} (corresponding to N-H bending), 1235 cm^{-1} (assigned to C-O stretching) and 1061 cm^{-1} (corresponding to C-N stretching) due to presence of amide bond revealing immobilization of Urs-GLDH onto nanocomposite. The weak bands seen at 1723 and 1812 cm^{-1} may perhaps be due to the formation of other intermediate compounds (acid derivative containing C=O group) as a result of reaction of nitric acid and water to the hydrocarbon chain of the precursor (titanium(IV) butoxide/zirconium (IV) n-propoxide).

The AFM image [Fig. 1C, (image a)] shows that $\text{TiO}_2\text{-ZrO}_2$ molecules are uniformly distributed onto the ITO surface resulting in rough nanoporous structure with average roughness of 0.67 nm . After co-immobilization of the enzymes (Urs and GLDH) (image b), the roughness increases to 3.81 nm revealing that nanoporous morphology of nanocomposite provides favorable environment for adsorption of enzymes. However, the average maximum height for $\text{TiO}_2\text{-ZrO}_2/\text{ITO}$ electrode increases from 11.9 to 21 nm after enzyme immobilization. The observed granular structure is due to aggregation of the enzyme molecules over the nanocomposite platform.

3.3 Electrochemical studies

Fig. 2A shows results of the cyclic voltammetric (CV) studies conducted on $\text{TiO}_2\text{-ZrO}_2/\text{ITO}$ electrode and Urs-GLDH/ $\text{TiO}_2\text{-ZrO}_2/\text{ITO}$ bioelectrode in phosphate buffer saline (PBS; 50 mM , $\text{pH } 7.0$, 0.9% NaCl) at constant flow rate. Typical CV of $\text{TiO}_2\text{-ZrO}_2$ nanocomposite [curve (i)] shows different peaks at lower potentials of 0.057 V and 0.0039 V (vs Ag/AgCl) due to anatase crystal (a band) and interfacial sites (s band) of TiO_2 (indicated by arrows a and s respectively) as reported in literature.^{17,18} Another broad oxidation peak found at higher potential 0.42 V is attributed to presence of ZrO_2 (indicated by arrow) in $\text{TiO}_2\text{-ZrO}_2$ nanocomposite.¹⁷ The oxidation peak current in curve (ii) is higher ($1.11 \times 10^{-6}\text{ A}$) and is shifted to the lower potential (0.334 V) after immobilization of Urs and GLDH onto transducer surface. This may perhaps be due to the fact that the $\text{TiO}_2\text{-ZrO}_2$ nanocomposite provides favorable microenvironment for enzymes (Urs and GLDH) that directly communicate with the active sites and establish an electron mediation path and hence lower the tunneling distance between active sites of enzymes and electrode surface resulting in enhanced magnitude of current. Moreover, small peak appears at higher current ($3.27 \times 10^{-7}\text{ A}$) and is shifted towards lower positive potential ($+0.03\text{ V}$) due to a band of TiO_2 system.

Cyclic voltammograms obtained for Urs-GLDH/ $\text{TiO}_2\text{-ZrO}_2/\text{ITO}$ bioelectrode as a function of scan rates ($20\text{--}100\text{ mVs}^{-1}$) have been shown in Fig. 2B. It is observed that the anodic

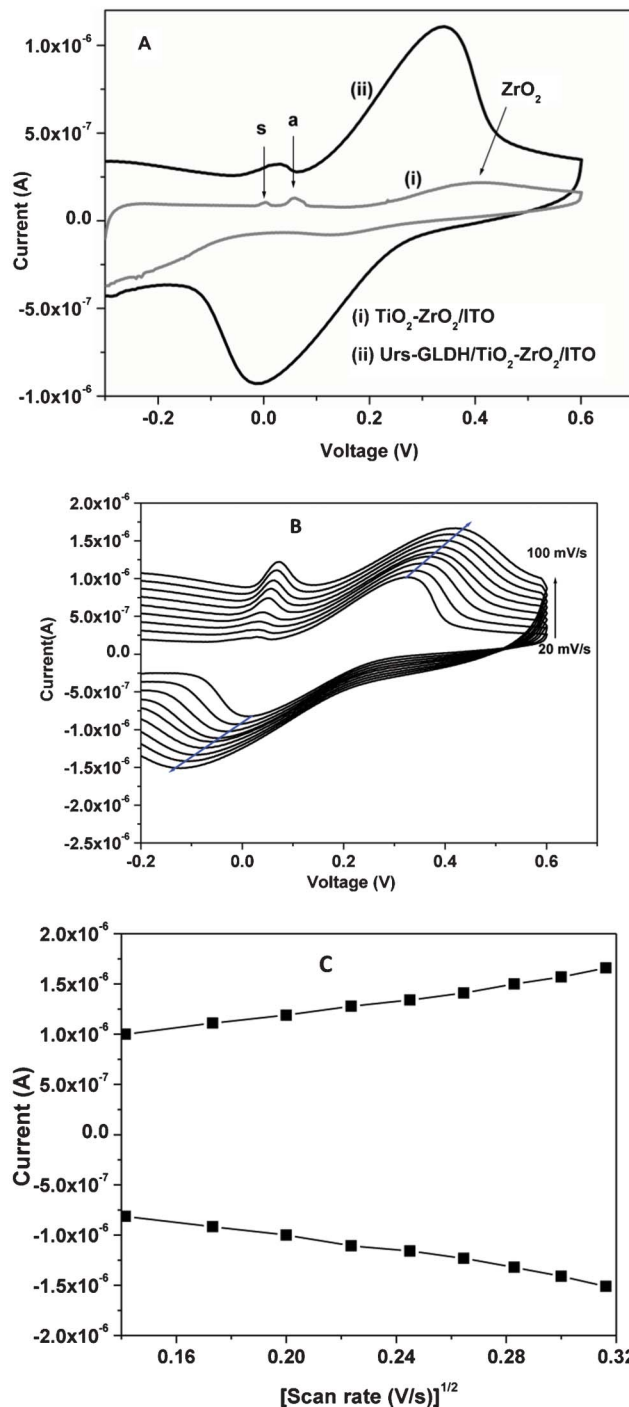


Fig. 2 (A) (i) Cyclic voltammetry (CV) of $\text{TiO}_2\text{-ZrO}_2/\text{ITO}$ electrode and (ii) Urs-GLDH/ $\text{TiO}_2\text{-ZrO}_2/\text{ITO}$ bioelectrode in PBS. (B) CV of Urs-GLDH/ $\text{TiO}_2\text{-ZrO}_2/\text{ITO}$ bioelectrode at different scan rates in PBS. (C) Magnitude of redox peak currents as a function of square root of scan rate.

potential shifts towards positive side and the cathodic peak potential shifts in the reverse direction (Fig. 2C), indicating a diffusion electron-transfer process follows eqn (3,4).

$$I_a = 4.63 \times 10^{-7} [\text{A}] + 3.68 \times 10^{-6} [\text{A}^2 \text{ mV}^{-1} \text{ s}]^{1/2} \times [\text{scan rate (mV s}^{-1})]^{1/2}, R^2 = 0.996 \quad (3)$$

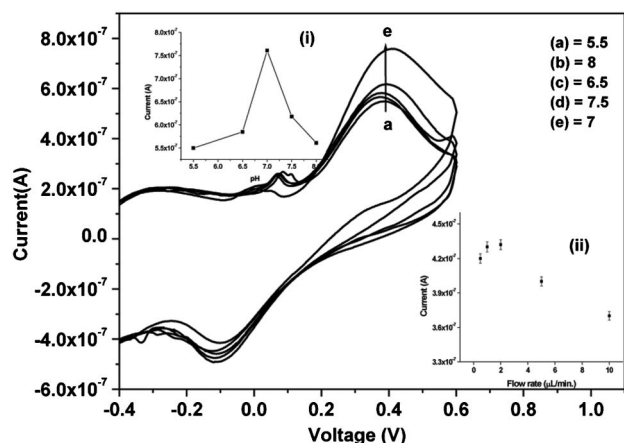


Fig. 3 CV response of Urs-GLDH/TiO₂-ZrO₂/ITO bioelectrode as a function of pH in PBS (5.5–8); inset (i): calibration curve between anodic peak current and pH value and inset (ii): shows the effect of flow rate on the response current

$$I_c = -2.41 \times 10^{-7} [A] - 3.87 \times 10^{-6} [A^2 \text{ mV}^{-1} \text{ s}]^{1/2} \times [\text{scan rate (mV s}^{-1})]^{1/2}, R^2 = 0.995 \quad (4)$$

The surface concentration of Urs-GLDH/TiO₂-ZrO₂/ITO bioelectrode estimated from plot of I_p versus scan rate (v) using the Brown-Anson model²¹ and found to be as $5.275 \times 10^{-12} \text{ mol cm}^{-2}$.

The effect of pH (5.5–8.0 at 25 °C) on the Urs-GLDH/TiO₂-ZrO₂/ITO bioelectrode has been investigated using CV to estimate optimum enzyme activity. The highest current (Fig. 3) is obtained at pH 7.0 revealing that bioelectrode is most active at this pH. Thus, all the experiments are carried out at pH of 7.0 and temperature of 25 °C. Inset (i) shows the anodic peak current as a function of pH using CV.

The variation of response current obtained as a function of flow rate (0.5, 1, 2, 5 and 10 $\mu\text{L min}^{-1}$) has been measured by taking 1 mM urea concentration injected into the micro-channel. It has been observed that the optimum flow rate is 2 $\mu\text{L min}^{-1}$ at which the response current is maximum [inset (ii); Fig. 3]. The parameters which affect the current response are flux of electro active species and retention time for the biochemical reaction. As we increase the flow rate, the retention time is found to be lesser resulting in decreased response current. It has been found that the flux is increased as flow rate increases, but at the same time, the retention time reduces beyond the optimum value of 2 $\mu\text{L min}^{-1}$. This is due to the fact that the biomolecules are shifted away from the microchannels before completing the biochemical reaction onto the sensor surface.

In the fluid mechanics, Reynolds number (R_e) is a dimensionless number that gives a measure of the ratio of inertial forces to viscous forces. The fluid flow through a microfluidics channels can be characterized by R_e defined in eqn (5)

$$R_e = \frac{\rho v L}{\mu} \quad (5)$$

where L is the characteristic length (200 μm) of channels, μ is

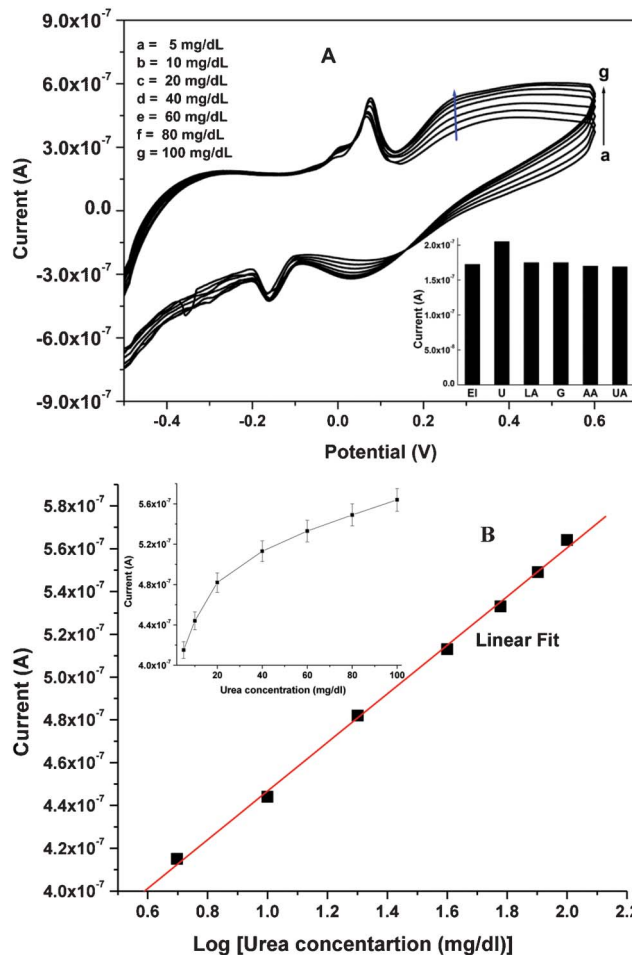
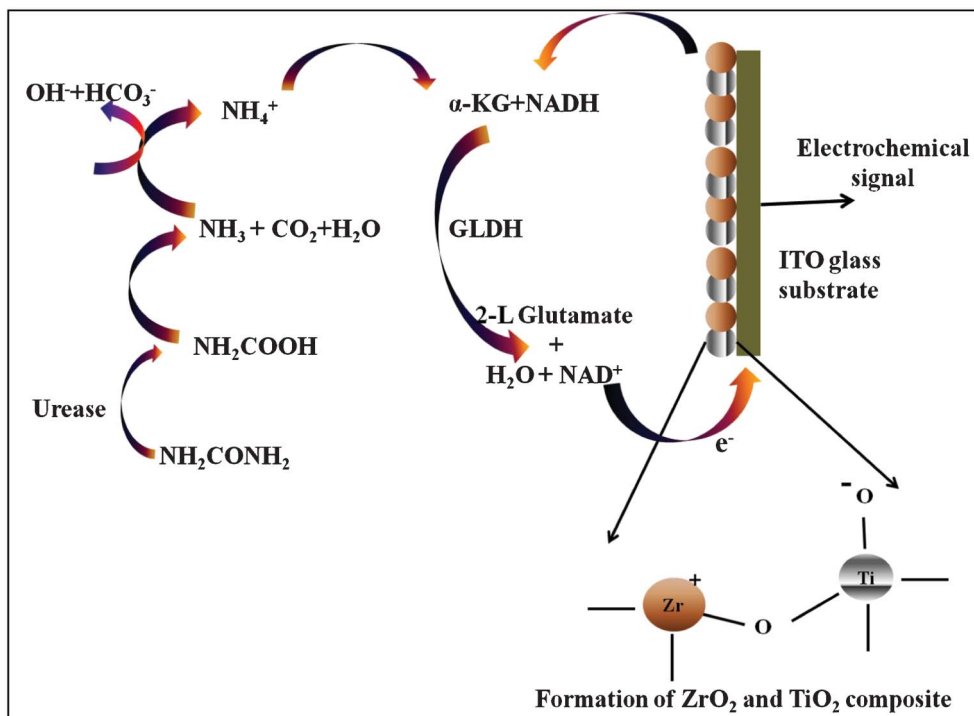


Fig. 4 (A) CV response of Urs-GLDH/TiO₂-ZrO₂/ITO bioelectrode as a function of urea concentration in PBS. Inset shows the effect of interferents (glucose, ascorbic acid, uric acid and lactic acid) on the current response of the Urs-GLDH/TiO₂-ZrO₂/ITO bioelectrode in PBS. (B) Calibration curve between response current and log urea concentration (5–100 mg/dl); inset (i) shows calibration curve between response current and urea concentration (5–100 mg/dl).

the viscosity (10^{-3} Pa s), v is average velocity of fluid ($0.083 \times 10^{-2} \text{ m s}^{-1}$) and ρ is fluid density (10^3 kg m^{-3}) from which the magnitude of R_e number comes out to be 0.166 indicating fluid flow is completely laminar and mass transfer occurs mainly by diffusion.

3.4 Electrochemical response studies

Electrochemical response studies of Urs-GLDH/TiO₂-ZrO₂/ITO bioelectrode have been conducted as a function of urea in presence of NADH and α -KG [Fig. 4A] in PBS, injected into the microchannels at continuous flow rate of 2 $\mu\text{L min}^{-1}$ using CV. The magnitude of response peak current increases as urea concentration increases. In proposed biochemical reaction (Scheme 3), urease catalyzes hydrolysis of urea to carbamate acid that gets hydrolyzed to ammonia (NH_3) and carbon dioxide (CO_2). GLDH catalyzes the reversible reaction between α -KG and NH_3 to NAD^+ and linked oxidative deamination of L-glutamate in two steps. The first step involves a Schiff base intermediate formed between NH_3 and α -KG (Step A). Then



Scheme 3 Showing biochemical reaction and electron transfer mechanism at the electrode surface.

Schiff base intermediate protonated due to transfer of the hydride ions from NADH resulting in formation of L-glutamate (Step B). NAD^+ is utilized in the forward reaction of α -KG and free NH_3 that is converted to L-glutamate *via* hydride transfer from NADH to glutamate. NAD^+ is utilized in the reverse reaction, involving L-glutamate being converted to α -KG and free (NH_3) *via* oxidative deamination reaction. The electrons generated during these reactions are transferred to TiO_2 - ZrO_2 /ITO electrode.

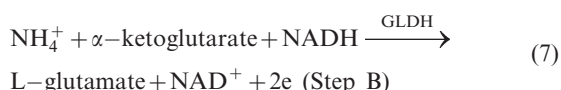


Fig. 4B shows the calibration plot between anodic peak current and log of urea concentration (5–100 mg/dL) and inset (i) shows the calibration plot between peak current *vs.* urea concentration (5–100 mg/dL). The lower detection limit is obtained as 0.07 mg/dL using the $3\sigma_b/m$ equation, where m is slope and σ_b is standard deviation of the calibration graph. The linear range is obtained as 5–100 mg/dl with sensitivity as $2.74 \mu\text{A} [\text{Log mM}]^{-1} \text{cm}^{-2}$. The higher sensitivity obtained as compared to reported data^{8,12,22,23} is not only due to the small geometry of microfluidics device, but also larger surface-to-volume ratio of nanocrystalline TiO_2 - ZrO_2 nanocomposite which increases surface density of enzyme loading. This microfluidics sensor for urea detection shows faster response time (10 s) attributed to small characteristic diffusion length towards microelectrode.

The shelf-life of the microfluidics sensor has been estimated by measuring electrochemical current response with respect to time, in a regular interval of 1 week. It is observed that this bioelectrode retains about 85% of the enzymes (Urs and

Table 1 Comparing sensing performance of the TiO_2 - ZrO_2 nanocomposite based microfluidics urea biosensor along with some of those reported in the literature

Bioelectrodes	Detection range (mM)	Detection limit (mM)	Sensitivity	Response time (s)	Microfluidics based	Ref.
Urs-GLDH/ZnO-Ch/ITO	0.8–16.6	0.49	$0.13 \mu\text{A mM}^{-1} \text{cm}^{-2}$	10	no	8
Urs/PAPCP/ITO	0.16–5.02	—	$0.47 \mu\text{A mM}^{-1} \text{cm}^{-2}$	40	no	22
Urs-GLDH/ ZrO_2 /ITO	0.8–16.6	0.8	$0.07 \mu\text{A mM}^{-1} \text{cm}^{-2}$	10	no	12
Urs-GLDH/Nano-ZnO/ITO	0.8–13.3	2.24	$8.7 \mu\text{A mM}^{-1} \text{cm}^{-2}$	—	no	24
EG-Ag-Z-Epoxy	0.2–1.4	0.05	$30 \mu\text{A mM}^{-1} \text{cm}^{-2}$	50	no	25
Urs-GLDH /CDT/Au	1.6–16.6	1.5	$7.5 \mu\text{A mM}^{-1} \text{cm}^{-2}$	10	yes	19
Ur-GLDH/ TiO_2 - ZrO_2 /ITO	0.8–16.6	0.44	$2.74 \mu\text{A mM}^{-1} \text{cm}^{-2}$	10	yes	Present work

GLDH) activity even after about 4 weeks when stored in refrigerated conditions (4 °C) after which the current response decreases to 80% in about 6 weeks (data not shown). The reproducibility of response of bioelectrode has been investigated using 10 mg/dL urea concentration. No significant decrease in current is observed after using at least 12 times.

The selectivity of Urs-GLDH/TiO₂-ZrO₂/ITO bioelectrode (EI) has been determined by comparing magnitude of the current response with individual normal concentration of interferents such as glucose (5 mM), ascorbic acid (0.05 mM), uric acid (0.1 mM) and lactic acid (5 mM) along with urea (1 mM) in PBS as shown in inset of Fig. 4A. Results of these studies indicate that the Urs-GLDH/TiO₂-ZrO₂/ITO bioelectrode is highly specific for the detection of urea only and exhibits negligible interference with other analytes.

The sensing performance of this TiO₂-ZrO₂ nanocomposite based microfluidics urea biosensor has been summarized in Table 1 along with those reported in the literature.

Conclusions

We have demonstrated the fabrication of a highly sensitive mediator-free microfluidics sensor comprising of PDMS microchannels, patterned electrodes for the rapid detection of urea. Urs and GLDH have been successfully co-immobilized onto TiO₂-ZrO₂ nanocomposite microelectrodes surface. This mediator-free microfluidics sensor offers improved sensitivity, detection limit and fast response time. This is attributed to the good electrocatalytic behavior of the nanocomposite as well as smaller geometry of the sensor. The reproducibility of bioelectrode has been investigated as 12 times. Efforts should be made to utilize this TiO₂-ZrO₂ nanocomposite microfluidics device for the estimation of other important analytes including cholesterol and low density lipoprotein.

Acknowledgements

We thank Director, National Physical Laboratory, New Delhi, India for providing the facilities. Saurabh Srivastava and Md. Azahar Ali are thankful to CSIR, India for the award of Senior Research Fellowship. Financial support received under the DST sponsored project (DST/TSG/ME/2008/18) is gratefully acknowledged. We are thankful to Mr. Sandeep Singh for AFM studies.

References

- 1 G. M. Whitesides, *Nature*, 2006, **442**, 368.
- 2 J. A. Wells, S. Vollmer, T. Bergman and H. Jornvall, *Anal. Biochem.*, 2005, **345**, 10.
- 3 B. S. Lee, Y. U. Lee, H. S. Kim, T. H. Kim, J. Park, J. G. Lee, J. Kim, H. Kim, W. G. Lee and Y. K. Cho, *Lab Chip*, 2011, **11**, 70.
- 4 Q. Xue, A. Wainright, S. Gangakhedkar and I. Gibbons, *Electrophoresis*, 2001, **22**, 4000.
- 5 G. M. Whitesides, E. Ostuni, S. Takayama, X. Jiang and D. E. Ingber, *Annu. Rev. Biomed. Eng.*, 2001, **3**, 335.
- 6 H. B.-Yoav, P. H. Dykstra, W. E. Bentley and R. Ghodssi, *Biosens. Bioelectron.*, 2012, **38**, 114.
- 7 P. R. Solanki, A. Kaushik, V. V. Agrawal and B. D. Malhotra, *NPG Asia Mater.*, 2011, **3**, 17.
- 8 A. Kaushik, P. R. Solanki, A. A. Ansari, G. Sumana, S. Ahmad and B. D. Malhotra, *Sens. Actuators, B*, 2009, **138**, 572.
- 9 P. R. Solanki, A. Kaushik, A. A. Ansari, G. Sumana and B. D. Malhotra, *Appl. Phys. Lett.*, 2008, **93**, 163903.
- 10 S. A. Kumar, P.H. Lo and S. M. Chen, *Nanotechnology*, 2008, **19**, 255501.
- 11 S. Liu, Z. Dai, H. Chen and H. Ju, *Biosens. Bioelectron.*, 2004, **19**, 963.
- 12 G. Sumana, M. Das, S. Srivastava and B. D. Malhotra, *Thin Solid Films*, 2010, **519**, 1187.
- 13 G. Dhawan, G. Sumana and B. D. Malhotra, *Biochem. Eng. J.*, 2009, **44**, 42.
- 14 B. Lakard, G. Herlem, S. Lakard, A. Antoniou and B. Fahys, *Biosens. Bioelectron.*, 2004, **19**, 1641.
- 15 Y. Velichkova, Y. Ivanov, I. Marinov, R. Ramesh, N. R. Kamini, N. Dimcheva, E. Horozova and T. Godjevargova, *J. Mol. Catal. B: Enzym.*, 2011, **69**, 168.
- 16 X. Wang, J. C. Yu, Y. Chen, L. Wu and X. Fu, *Environ. Sci. Technol.*, 2006, **40**, 2369.
- 17 K. L. Frindell, J. Tang, J. H. Harreld and G. D. Stucky, *Chem. Mater.*, 2004, **16**, 3524.
- 18 D. Keomany, J. P. Petit and D. Deroo, *Sol. Energy Mater. Sol. Cells*, 1995, **36**, 397.
- 19 S. Srivastava, P. R. Solanki, A. Kaushik, Md. A. Ali, A. Srivastava and B. D. Malhotra, *Nanoscale*, 2011, **3**, 2971.
- 20 B. M. Reddy and B. Chowdhury, *J. Catal.*, 1998, **179**, 413.
- 21 A. J. Bard and L. R. Faulkner, *Electrochemical Methods: Fundamentals and Applications*, 2nd ed., Wiley, New York.
- 22 V. Rajesh, W. Bisht, W. Takashima and K. Kaneto, *Biomaterials*, 2005, **26**, 3683.
- 23 J. M. C. S. Magalhaes and A. A. S. C. Machado, *Talanta*, 1998, **47**, 191.
- 24 A. Ali, A. A. Ansari, A. Kaushik, P. R. Solanki, A. Barik, M. K. Pandey and B. D. Malhotra, *Mater. Lett.*, 2009, **63**, 2473.
- 25 F. Manea, A. Pop, C. Radovan, P. Malchev, A. Bebeselea, G. Burtica, S. Picken and J. Schoonman, *Sensors*, 2008, **8**, 5806.